

Atmospheric ammonia in urban and remote regions

Beatriz Herrera^{1,2}, Kimberly Strong², Michel Grutter³, Wolfgang Stremme³, Camille Viatte⁴

¹ Department of Physical and Environmental Sciences, University of Toronto, Toronto, Canada

² Department of Physics, University of Toronto, Toronto, Canada

³ Centro de Ciencias de la de la Atmósfera, Universidad Nacional Autónoma de Mexico (UNAM), Mexico City, Mexico

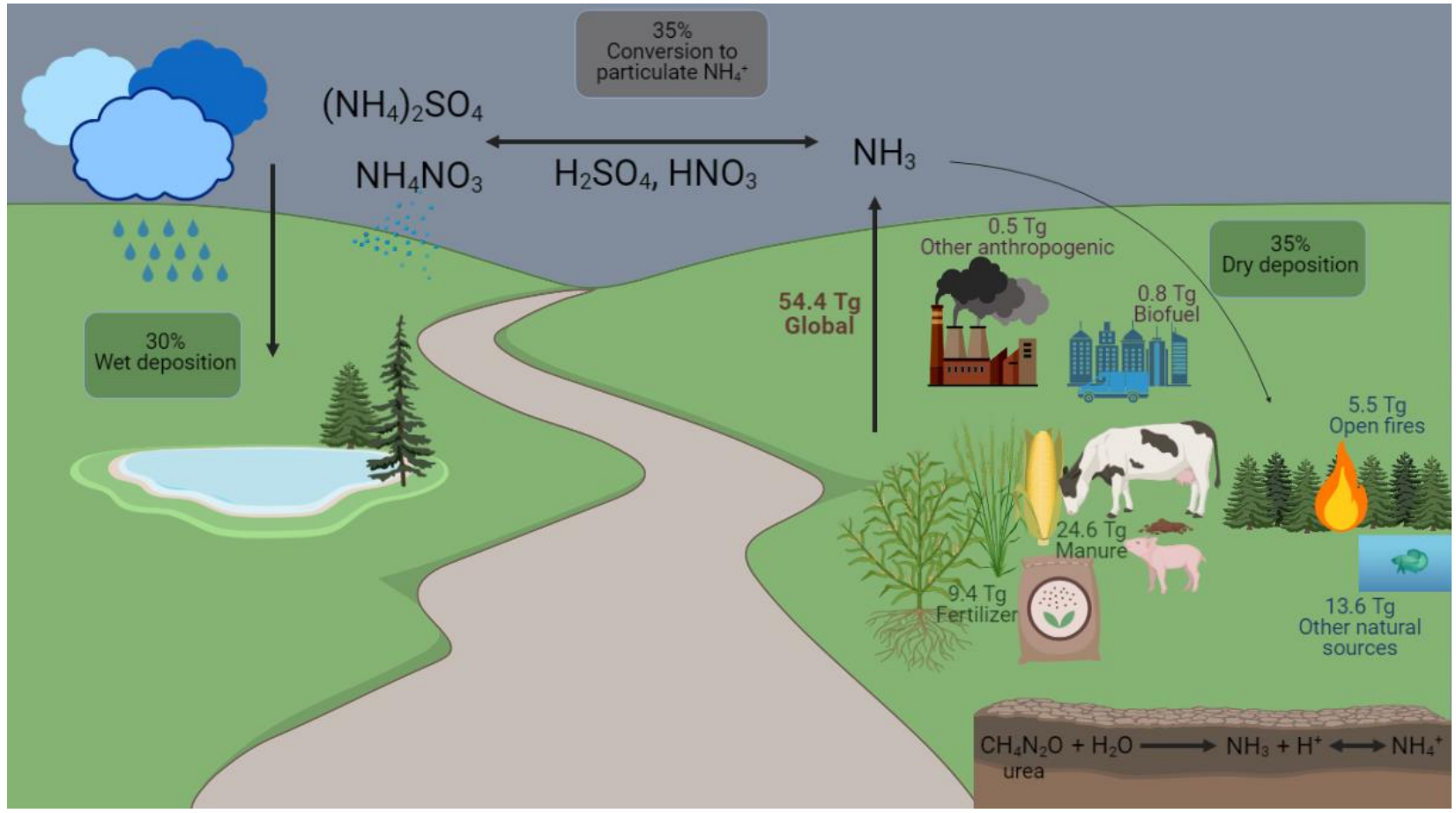
⁴ LATMOS/IPSL, Sorbonne Université, UVSQ, CNRS, Paris, France.

Contact: beatriz.herrera@mail.utoronto.ca

NDACC – IRWG Online meeting

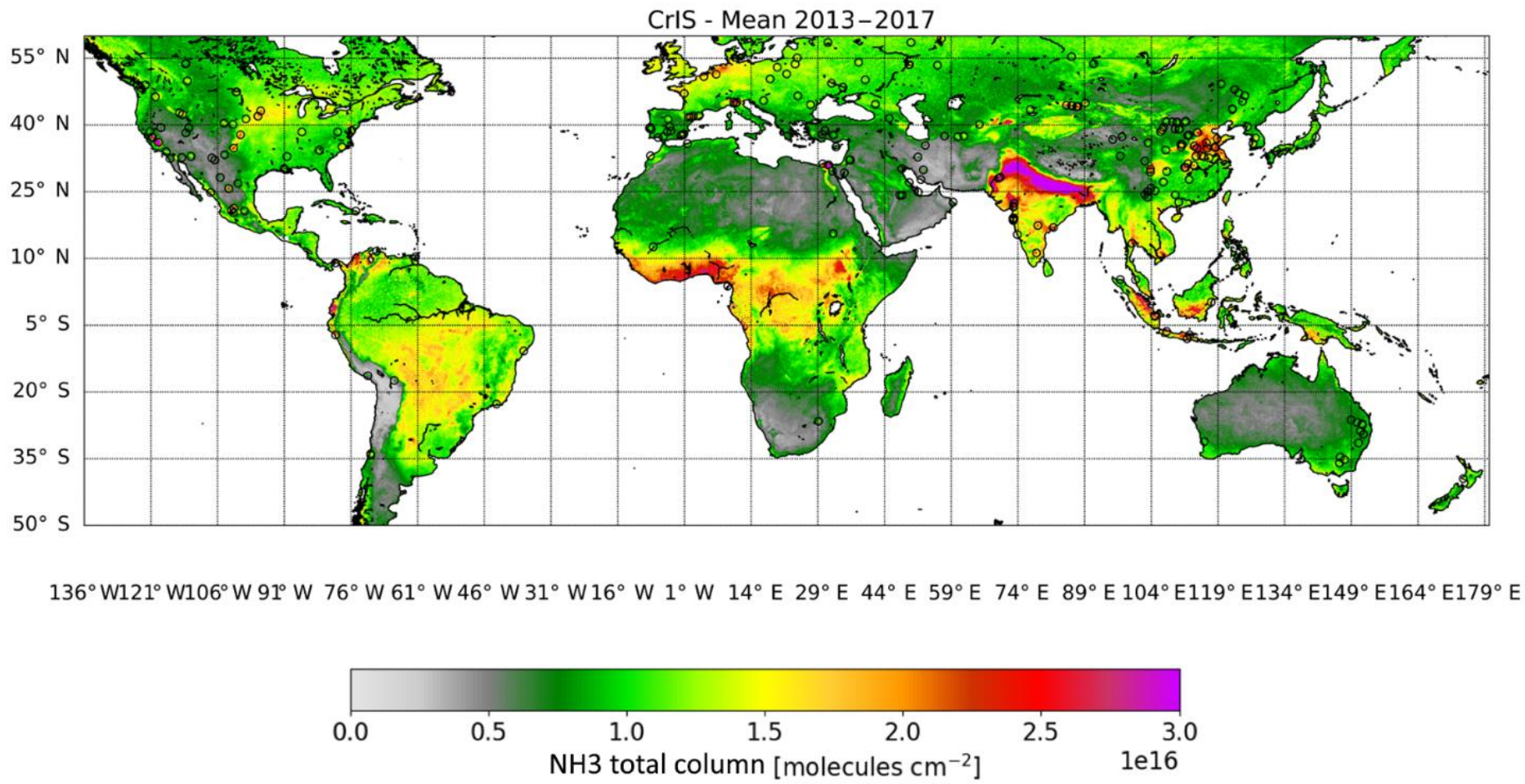
June 2021

Background - Atmospheric Ammonia (NH_3)



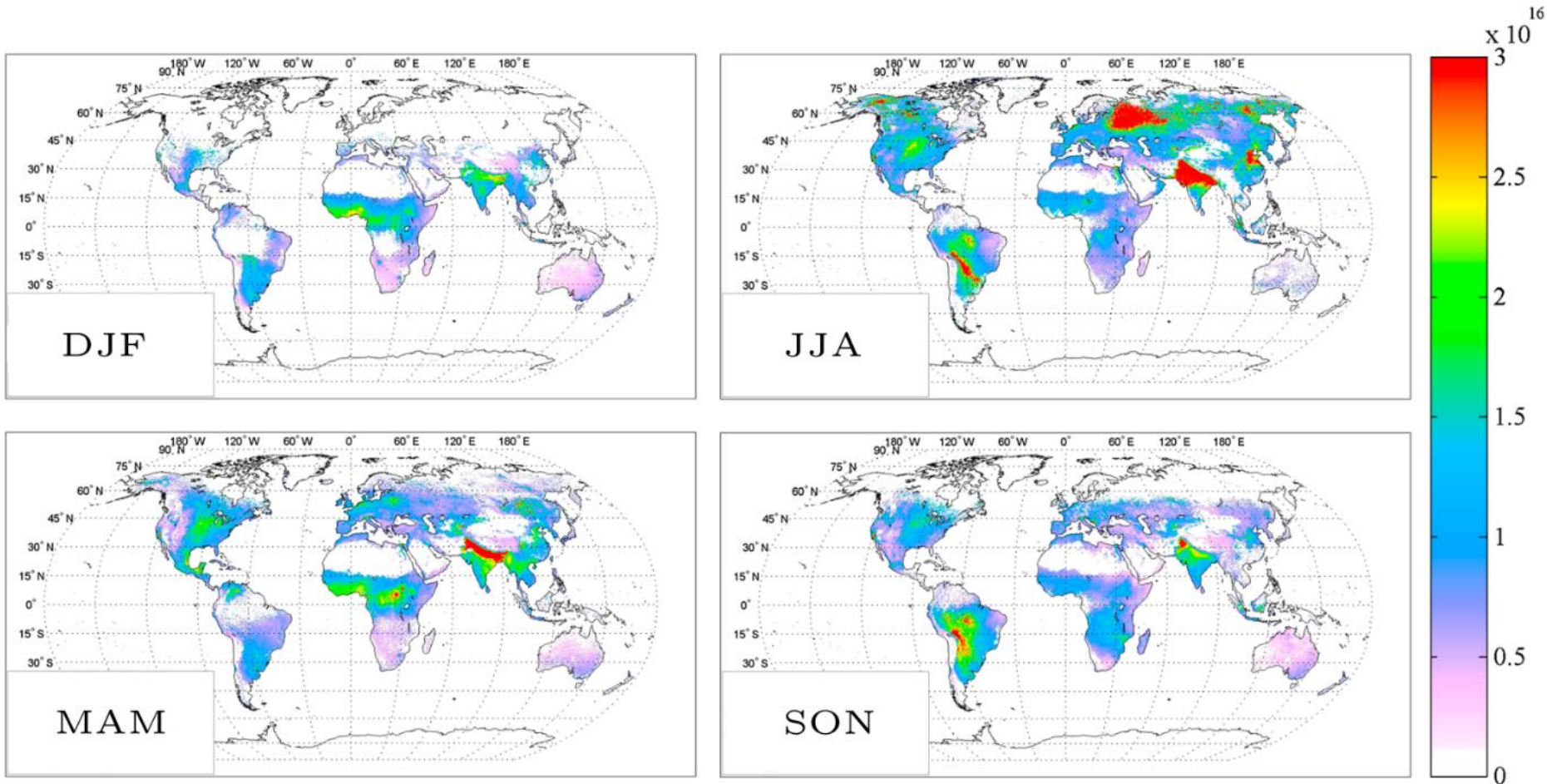
Atmospheric NH_3 : main chemical reactions, global emissions and sources, and global budget. The emission values are mostly for 2005 -2008 (Paulot et al., 2014). The global depositions and conversion to particulate NH_4^+ percentages are from model simulations (Khan et al., 2020).

Background - NH₃ Distribution



Global 5-year mean (2013-2017) of CrIS NH₃ total columns distribution at 0.05° x 0.05° (long, lat) resolution (Dammers et al., 2019).

Background - NH₃ Variability



Global 6-year (2008-2013) weighted mean distribution of seasonal total columns of NH₃ (molecules/cm², vertical color bar) from IASI morning measurements in 0.25° x 0.5° cells. December-January-February (DJF), March-April-May (MAM), June-July-August (JJA), and September-October-November (SON). Modified from Van Damme et al., (2015).

Background - NH₃ in the Arctic

NH₃ sources: hydrolysis of guano from migratory seabirds (Blackall *et al.*, 2007; Croft *et al.*, 2016; Riddick *et al.*, 2012; Sutton *et al.*, 2013; Wentworth *et al.*, 2016), seal excreta (Theobald *et al.*, 2006), and the ice-free and snow-free tundra (Croft *et al.*, 2019)

NH₃ enhancements due to boreal wildfires in the Northwest Territories have also been observed (Wentworth *et al.*, 2016, Lustch *et al.*, 2019)



Arctic fox at Eureka, 2020

Objectives

To improve our knowledge of NH_3 in urban and remote regions by using FTIR measurements, satellite data, and a chemical transport model.



1) Variability and trends of NH_3 using ground-based FTIR data

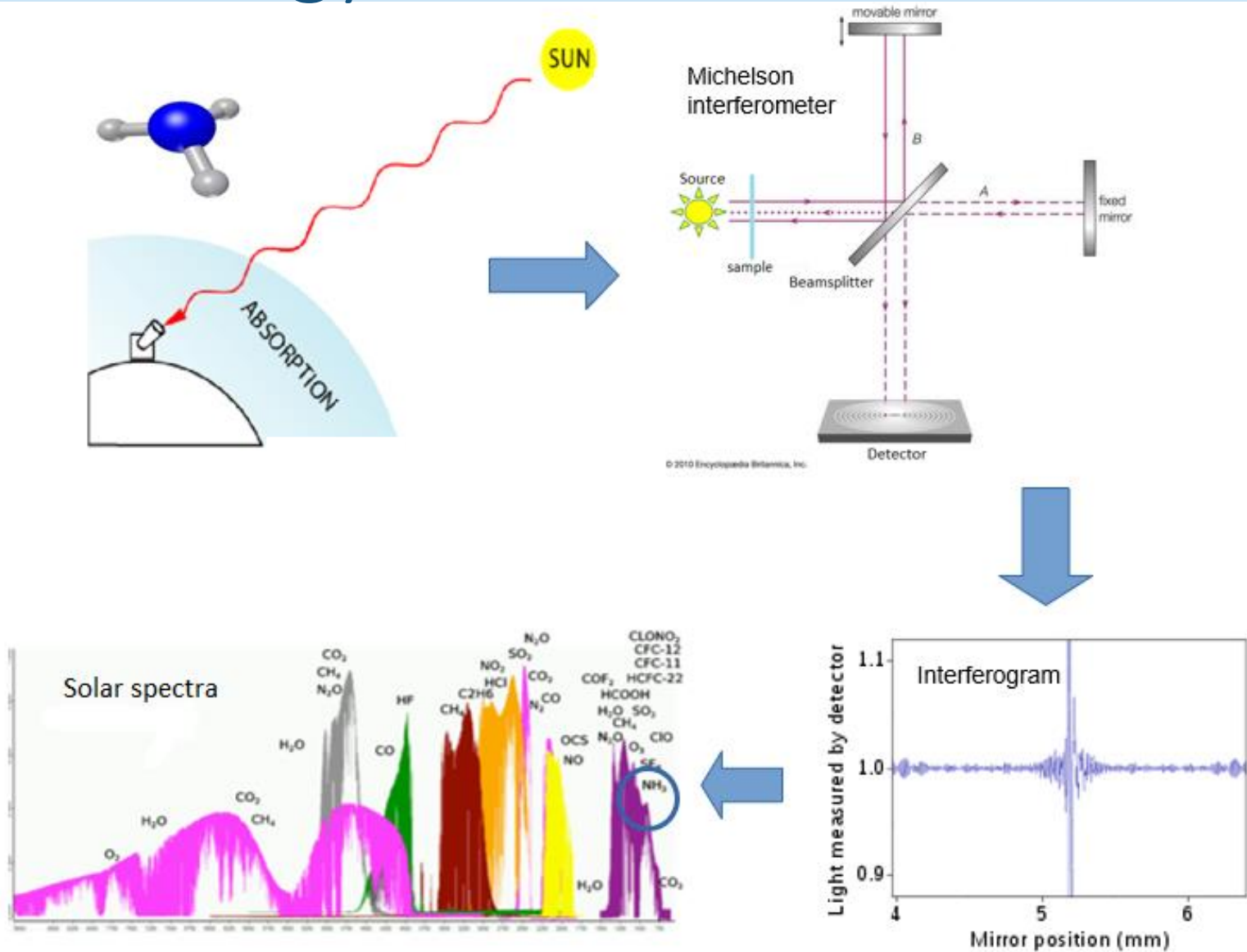


2) Link between NH_3 and $\text{PM}_{2.5}$ formation in Mexico City



3) Long-term impacts of boreal wildfire NH_3 on the Arctic

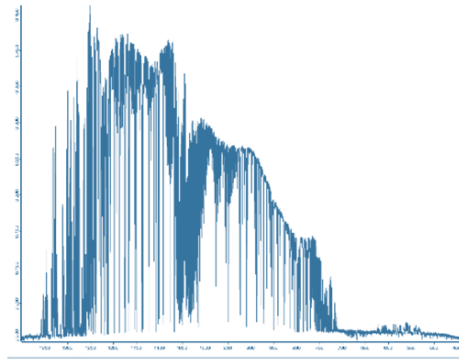
Methodology - FTIR



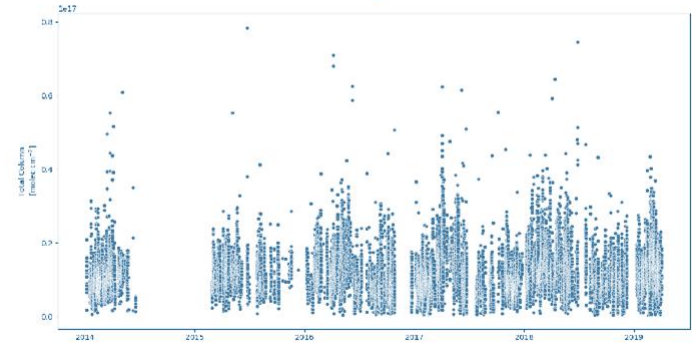
Basic elements of a solar FTIR experiment (Michelson interferometer adapted from Encyclopedia Britannica).

Methodology - SFIT4

SFIT4 is based on the SFIT2 algorithm, which is built upon the Optimal Estimation Method (OEM) from Rodgers (2000). The SFIT4 retrieval strategy minimize the difference between the measured spectrum and a theoretical calculated one (Pougatchev & Connor, 1995).



SFIT4 →

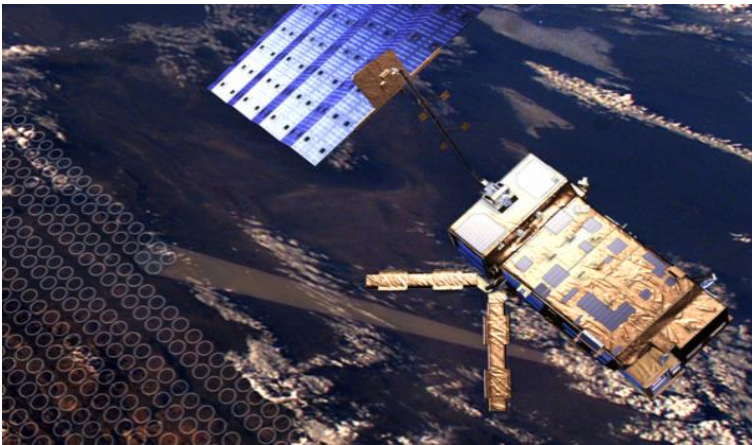


Parameter	
Microwindow 1	930.32 – 931.32 cm ⁻¹
Microwindow 2	966.97 – 970.0cm ⁻¹
Interfering species	H ₂ O, O ₃ , CO ₂ , N ₂ O, HNO ₃
SFIT4 version	V0.9.4.4

Methodology

Satellite Data

IASI is a spectrometer on board the meteorological satellite platforms MetOp, that measures infrared thermal radiation emitted by the Earth's surface and the atmosphere in a range of 2760 to 645 cm^{-1} . (Shepard and Cady-Pereira, 2015).



IASI onboard the MetOp satellite, image from ESA.

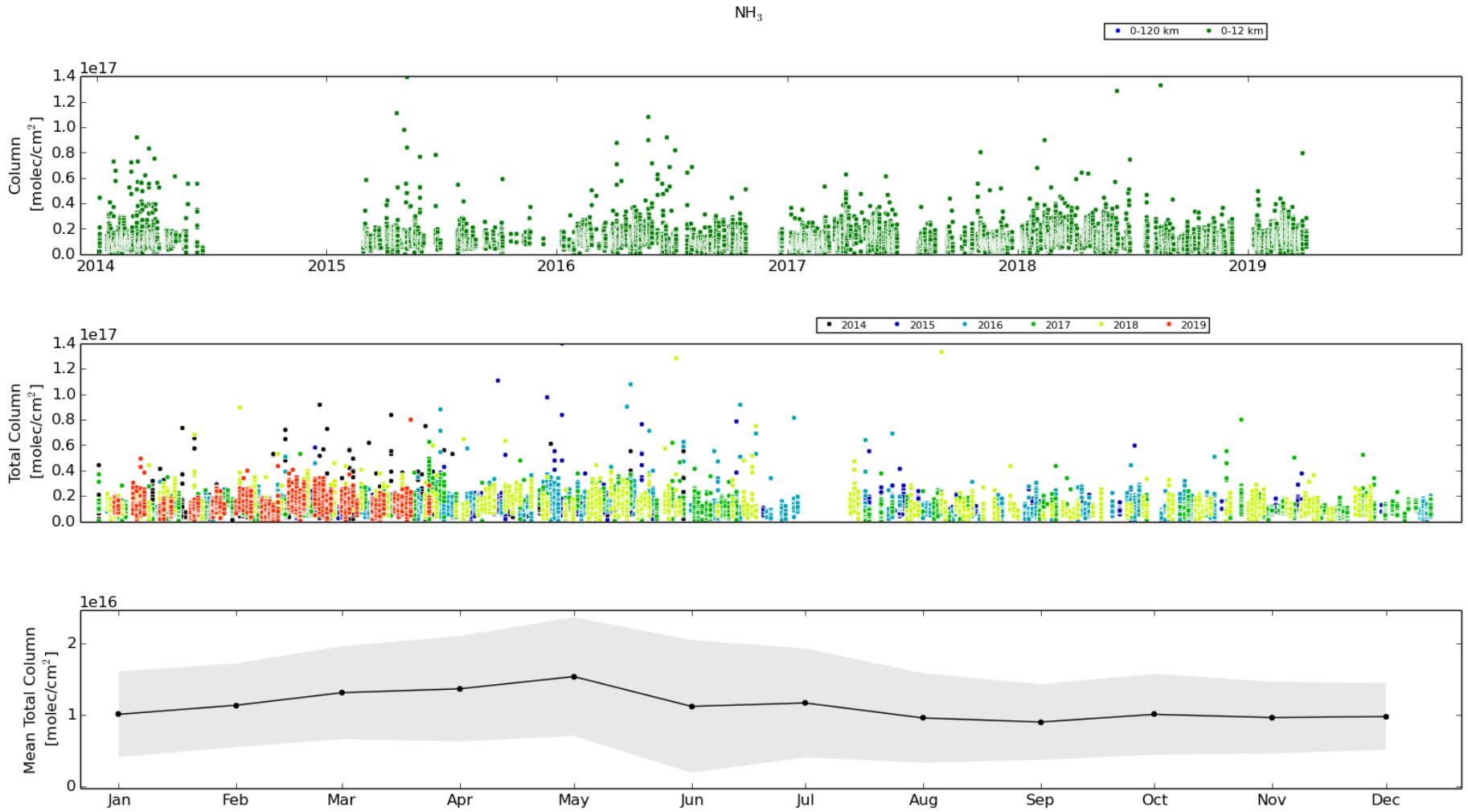
Atmospheric Models

Is a global 3-D model of atmospheric chemistry with assimilated meteorology from the Goddard Earth Observing System (GEOS) of the NASA (Bey et al., 2001)

Core -> chemical module that computes the local changes in atmospheric concentrations due to emissions, chemistry, aerosol microphysics and deposition (www.geos-chem.org)

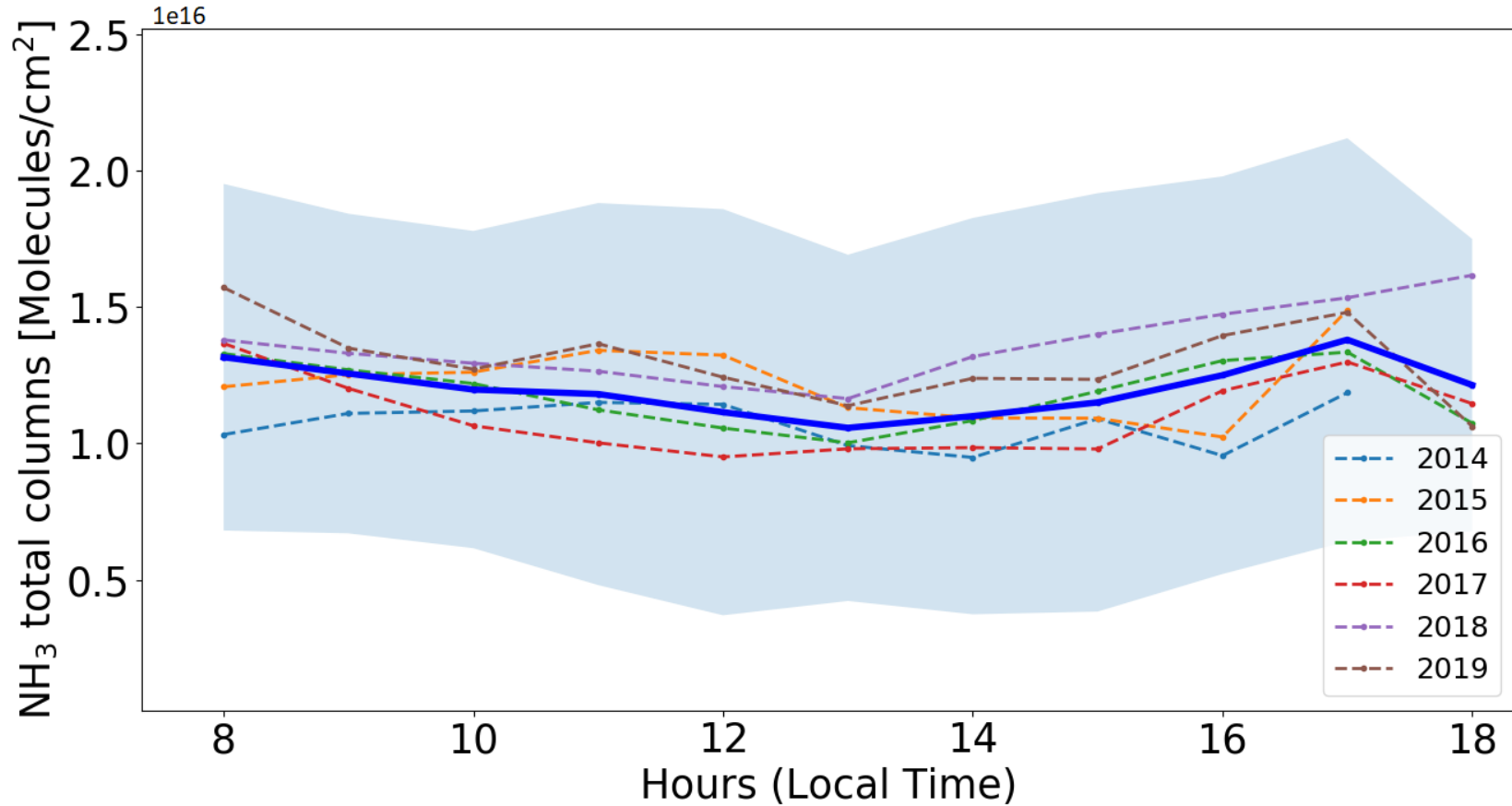
GEOS-Chem

Preliminary Results – Mexico City



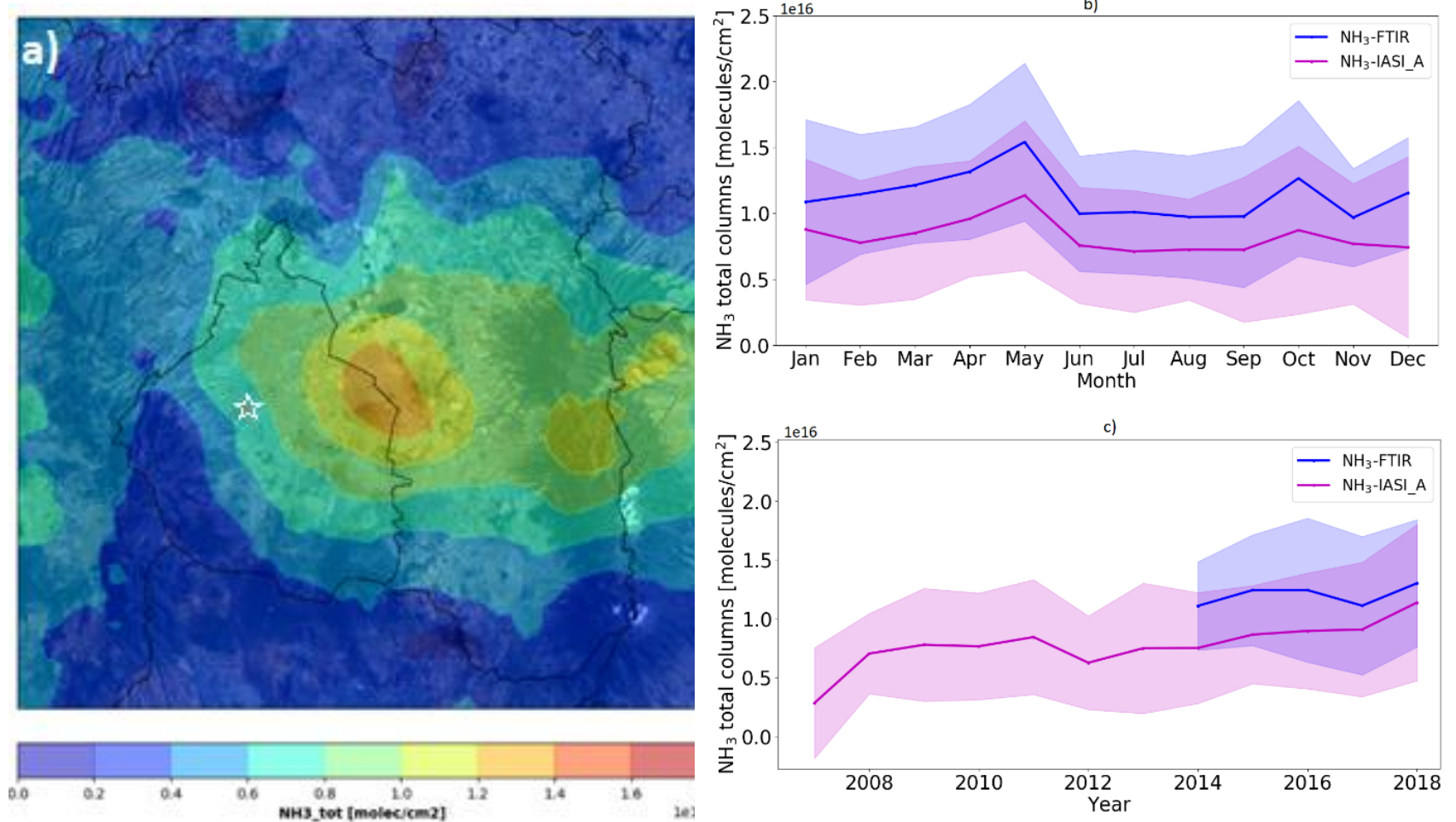
Time series of NH₃ total columns at Mexico City (UNAM) station between January 2014 and April 2019. Time series but all years are plotted in different colors while the monthly means are in the bottom panel to show the seasonal variability of NH₃. The gray shaded area in the monthly means indicate 1σ from the monthly mean. The mean NH₃ column is $1.21 \times 10^{16} \pm 8.86 \times 10^{15}$ molecules cm⁻², the mean DOFS is 0.86 ± 0.07 .

Mexico City



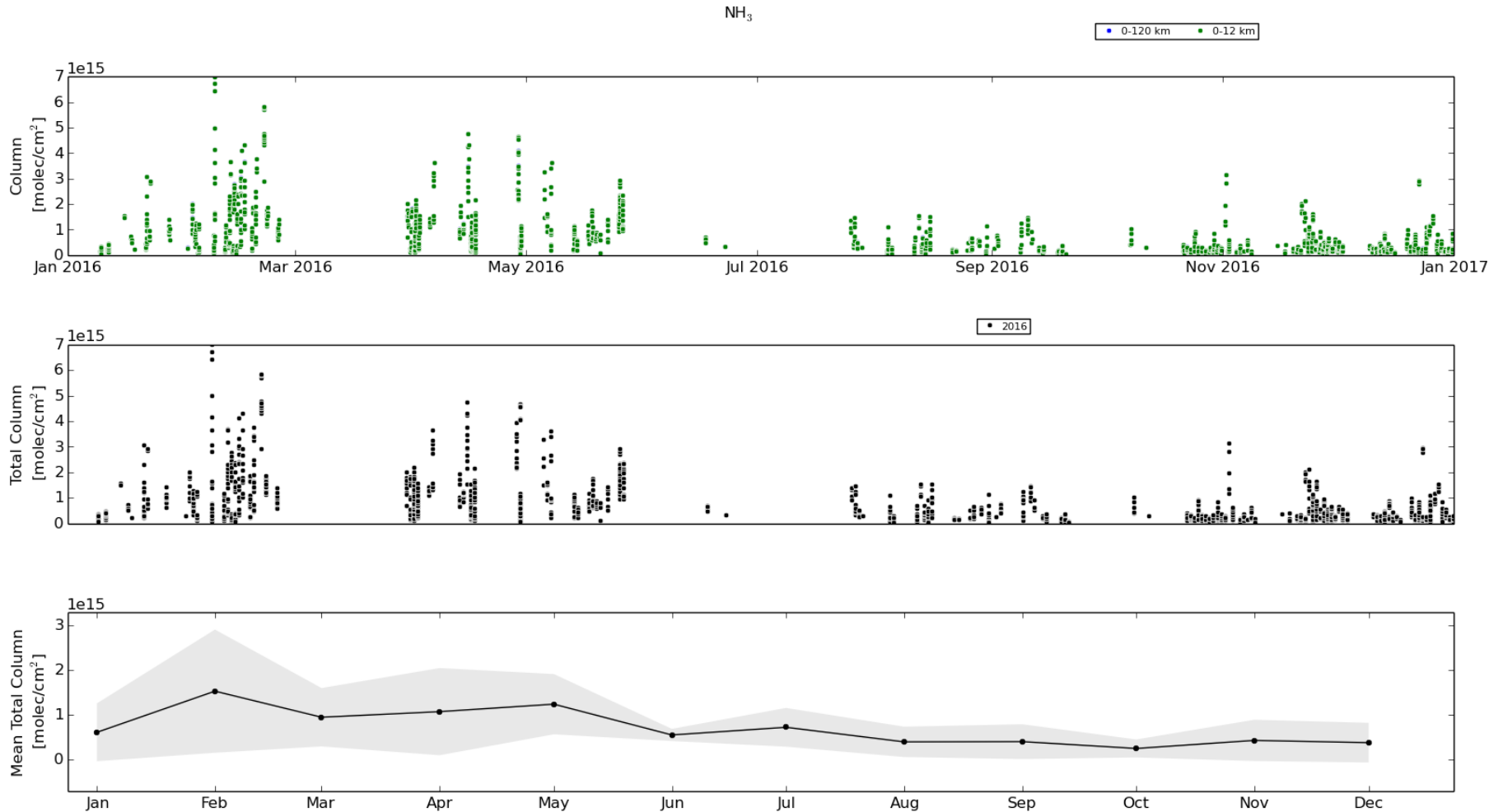
6-year (2014-2019) mean diurnal pattern of NH_3 total columns over Mexico City. The thick blue line is the average for all years and the blue shaded area indicates 1σ from the hourly mean.

Mexico City



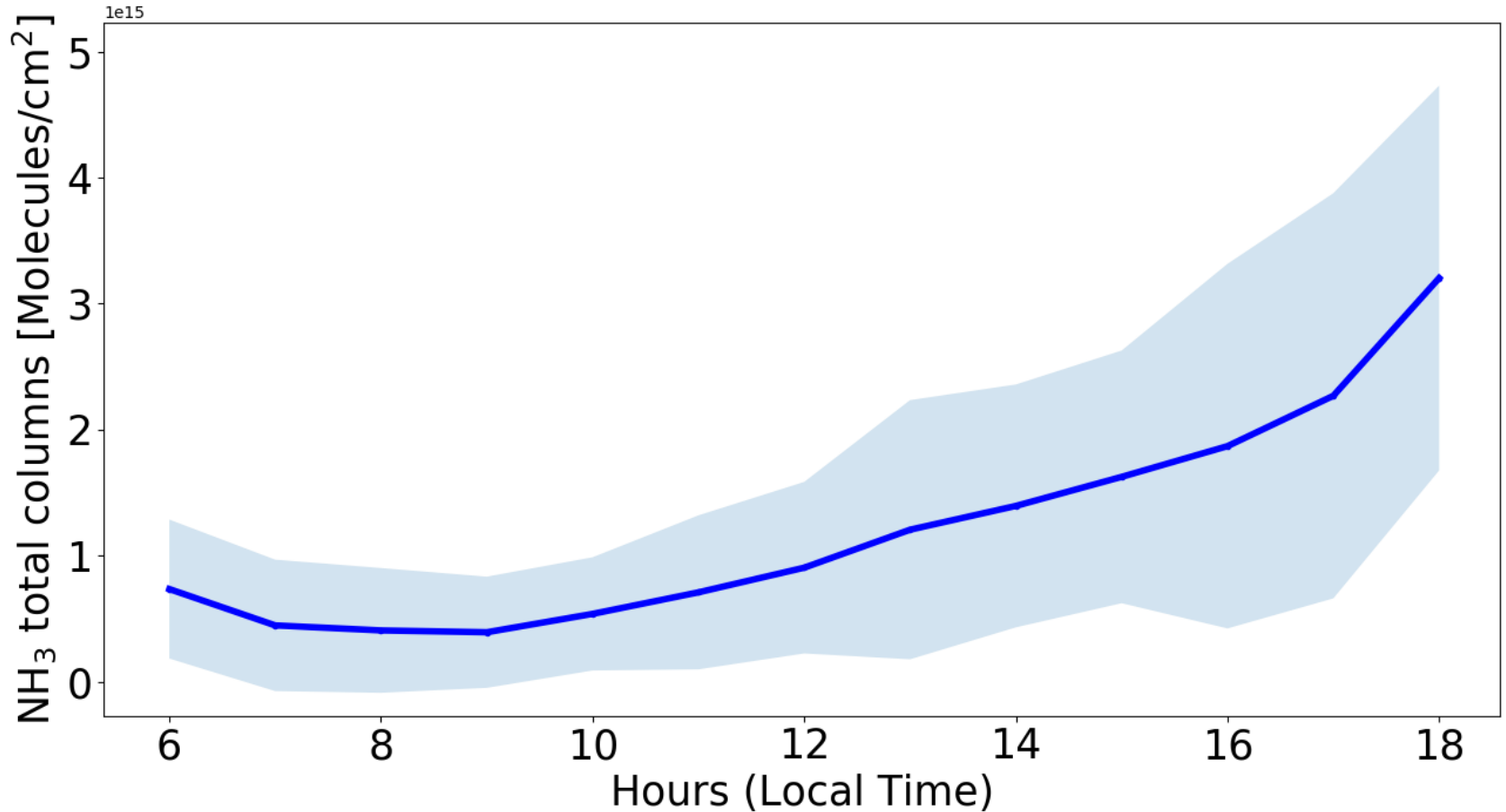
a) Average spatial distribution of NH_3 total columns over Mexico City measured by IASI-A between 2007-2018. The white star shows the location of the UNAM station in Mexico City. The IASI data version used is ANNI- NH_3 -v3, provided by the ULB/LATMOS team. The figures on the right show NH_3 total columns from ground-based FTIR measurements at UNAM and satellite measurements from IASI-A monthly (b) and annual (c) averages. The shaded area indicates 1σ from the monthly and annual mean.

Altzomoni



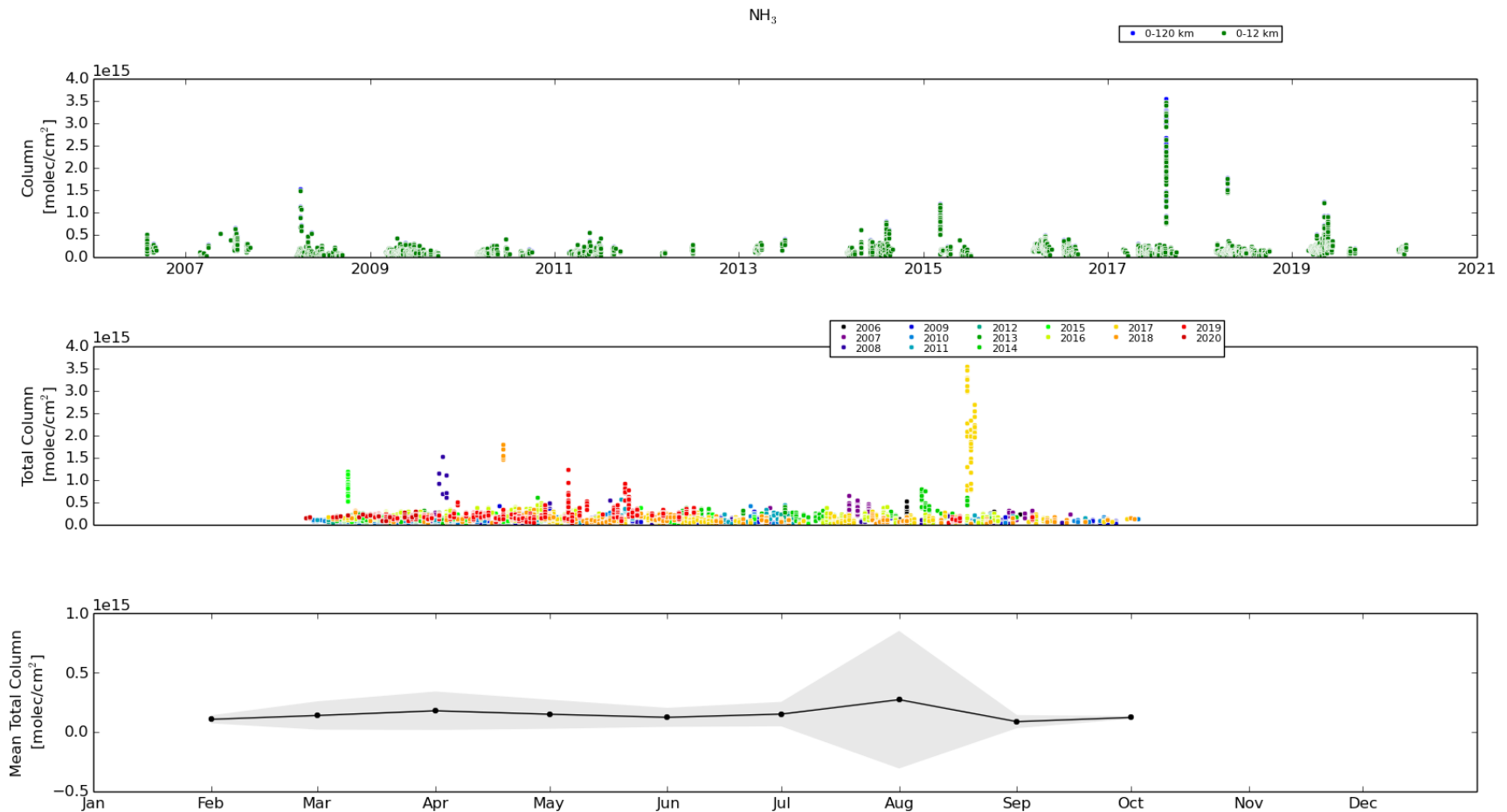
Time series of NH_3 total columns at Altzomoni station between January – December 2016. Time series but all years are plotted in different colors while the monthly means are in the bottom panel to show the seasonal variability of NH_3 . The mean NH_3 column is $5.84 \times 10^{14} \pm 6.80 \times 10^{14}$ molecules cm^{-2} , the mean DOFS is 0.76 ± 0.31 .

Altzomoni



1-year (2016) mean diurnal pattern of NH₃ total columns over Altzomoni. The blue shaded area indicates 1σ from the hourly mean. The bottom panel in black indicates the monthly means and the gray shaded area indicates 1σ from the monthly mean.

Eureka



Time series of NH_3 total columns at Eureka station between August 2006 and March 2020. Time series but all years are plotted in different colors while the monthly means are in the bottom panel to show the seasonal variability of NH_3 . The mean NH_3 column is $1.69e14 \pm 2.41e14$ molecules cm^{-2} , the mean DOFS is 0.96 ± 0.14 .

Future work



Study sites locations, green for remote sites and blue for urban sites, image from the NDACC IRWG website.

- Retrieval strategies
- Acquisition of NH_3 satellite data
- Acquisition of NH_3 time series
- Variability and trends
- Model simulation



Acknowledgements



Consejo Nacional de Ciencia y Tecnología



UNIVERSITY OF
TORONTO



References

- Khan, M. A. H., Lowe, D., Derwent, R. G., Foulds, A., Chhantyal-Pun, R., McFiggans, G., Orr-Ewing, A. J., Percival, C. J., & Shallcross, D. E. (2020). Global and regional model simulations of atmospheric ammonia. *Atmospheric Research*, 234(September 2019), 104702. <https://doi.org/10.1016/j.atmosres.2019.104702>
- Paulot, F., Jacob, D. J., Pinder, R. W., Bash, J. O., Travis, K., & Henze, D. K. (2014). Ammonia emissions in the United States, European Union, and China derived by high-resolution inversion of ammonium wet deposition data: Interpretation with a new agricultural emissions inventory (MASAGE_NH3). *Journal of Geophysical Research*, 119(7), 4343–4364. <https://doi.org/10.1002/2013JD021130>
- Dammers, E., McLinden, C. A., Griffin, D., Shephard, M. W., Van Der Graaf, S., Lutsch, E., Schaap, M., Gainairu-Matz, Y., Fioletov, V., Van Damme, M., Whitburn, S., Clarisse, L., Cady-Pereira, K., Clerbaux, C., François Coheur, P., & Erismann, J. W. (2019). NH3 emissions from large point sources derived from CrIS and IASI satellite observations. *Atmospheric Chemistry and Physics*, 19(19), 12261–12293. <https://doi.org/10.5194/acp-19-12261-2019>
- Van Damme, Martin, Erismann, J. W., Clarisse, L., Dammers, E., Whitburn, S., Clerbaux, C., Dolman, A. J., & Coheur, P. (2015). Worldwide spatiotemporal atmospheric ammonia (NH3). *Geophys. Res. Lett.*, 42, 1–9. <https://doi.org/10.1002/2015GL065496>
- Pöschl, U. (2005). Atmospheric aerosols: Composition, transformation, climate and health effects. *Angewandte Chemie - International Edition*, 44(46), 7520–7540. <https://doi.org/10.1002/anie.200501122>
- Pougatchev, N.S., Connor, B.J., R. C. P. (1995). Infrared measurements of the ozone vertical distribution above Kitt Peak. *Journal of Geophysical Research*, 100, 16689–16697.
- Shephard, M. W., & Cady-Pereira, K. E. (2015). Cross-track Infrared Sounder (CrIS) satellite observations of tropospheric ammonia. *Atmospheric Measurement Techniques*, 8(3), 1323–1336. <https://doi.org/10.5194/amt-8-1323-2015>
- Bey, I., Jacob, D. J., Yantosca, R. M., Logan, J. A., Field, B. D., Fiore, A. M., Li, Q., Liu, H. Y., Mickley, L. J., & Schultz, M. G. (2001). Global modeling of tropospheric chemistry with assimilated meteorology: Model description and evaluation. *Journal of Geophysical Research Atmospheres*, 106(D19), 23073–23095. <https://doi.org/10.1029/2001JD000807>
- Wen, D., Lin, J. C., Millet, D. B., Stein, A. F., & Draxler, R. R. (2012). A backward-time stochastic Lagrangian air quality model. *Atmospheric Environment*, 54, 373–386. <https://doi.org/10.1016/j.atmosenv.2012.02.042>